Nonlinear charging effect of quantum dots in a *p-i-n* diode

G. Kießlich,* A. Wacker, and E. Schöll
Institut für Theoretische Physik, Technische Universität Berlin, D-10623 Berlin, Germany

S. A. Vitusevich,[1,†] A. E. Belyaev,[1,2] S. V. Danylyuk,[3] A. Förster,[1] N. Klein,[1] and M. Henini[2]
[1]*Institut für Schichten und Grenzflächen, Forschungszentrum Juelich, D-52425 Juelich, Germany*
[2]*School of Physics and Astronomy, University of Nottingham, NG7 2RD, Nottingham, United Kingdom*
[3]*Institute of Semiconductor Physics, NASU, 03028 Kiev, Ukraine*

(Received 20 November 2002; revised manuscript received 5 May 2003; published 29 September 2003)

The current through a *p-i-n* diode containing a layer of self-assembled InAs quantum dots in the intrinsic region is investigated. A series of peaks is observed in the differential conductance below the flat band regime which we attribute to electron tunneling in the quantum dot and wetting layer states, combining the carrier recombination and the carrier relaxation effects. This phenomenon is investigated numerically on the basis of a master equation model. Criteria for the observability of the charging of individual quantum dots are discussed. A key point is the presence of Coulomb screening as otherwise the long-range interdot interactions smear out the energy level spectrum.

DOI: 10.1103/PhysRevB.68.125331 PACS number(s): 73.23.Hk, 73.50.Gr, 73.63.Kv

I. INTRODUCTION

The investigation of charging effects in tunneling transport through small quantum dots (QD's) has opened up a large research field in the last decade. Particularly, in the nonlinear regime the current-voltage characteristic of a tunneling device containing a single QD exhibits steplike structures, known as the Coulomb staircase (for a review see Refs. 1–3). Most of these experiments and theories are restricted to unipolar electronic transport through single or only few coupled QD's. With the facility of fabrication of large ensembles of self-organized QD's, tunneling experiments through such QD arrays were reported.[4–6] In the present paper we investigate the bipolar transport through an array of self-organized QD's and show that charging effects of QD's are revealed in the current-voltage characteristics. For unipolar transport through single QD's a master equation model is available,[7–9] which we extended for large QD arrays[10,11] and for the case where electrons and holes contribute to the current in order to interpret our experimental data (see Ref. 12). Here we investigate a double barrier AlAs/GaAs/AlAs structure incorporated in the intrinsic *i* region of a GaAs *p-i-n* diode. Additionally, a layer of InAs self-organized QD's is embedded in the center of the GaAs quantum well (QW). The presence of these QD states and wetting layer (WL) states gives rise to a current flow for voltages below the flat band condition due to the combined effects of tunneling, carrier recombination, and carrier relaxation processes. This is confirmed by reproducible differential conductance peaks which are caused by the successive charging of many-particle states in the QD ensemble. We discuss a model that explains the appearance of these oscillations and investigate how Coulomb interaction between carriers in the QD ensemble as well as size fluctuations of the individual QD's influence the observability of the conductance oscillations.

Double barrier resonant tunneling structures (DBRT) embedded in the intrinsic region of an *n-i-n* diode represent a well-known nonlinear system that shows *N*- (or in some cases *Z*-) shaped current-voltage characteristics.[13–16] Asymmetric design of barriers provides large charge accumulation inside the QW, and a hysteresis loop is observed when the voltage is swept up and down.[17,18] A giant *Z*-shaped bistability has also been observed if the charge accumulation occurs in a triangular well that is formed in front of the emitter barrier.[19] In contrast to these standard unipolar devices, DBRT embedded in the intrinsic region of a *p-i-n* diode can give rise to a *S*-shaped current-voltage characteristic and, consequently, show inverted current bistability due to different rates for electron and hole injection in and escape out the QW.[20–22] For our device a combination of both *S*- and *Z*-shaped current bistability in the current-voltage characteristic is observed.

II. EXPERIMENTAL SETUP

The sample is a *p-i-n* structure grown by molecular beam epitaxy on a n^+GaAs substrate. The structure incorporates two 3-nm AlAs barriers and a 6.2-nm GaAs QW in the undoped intrinsic *i* region. Undoped spacer layers of 100 nm (60 nm) separate the barriers from 2×10^{16} cm^{-3} *n*-doped (2×10^{18} cm^{-3} *p*-doped) contact layers (see Fig. 1). A 1.8-monolayer (ML) plane of InAs is embedded in the middle of QW to form a plane of QD's (density: 10^{10}–10^{11} cm^{-2}). The structure was grown at 600 °C except for the InAs layer and the overgrown GaAs cap layer, which were both grown at 450 °C to avoid In segregation and desorption effects. A schematic diagram of the DBRT in the intrinsic region is shown in the inset of Fig. 1 where the electron/hole QW states are labeled. The electron and hole levels in the QW were assigned on the basis of a self-consistent solution of Schrödinger and Poisson equations taking into account a thin InAs layer in the middle of the QW.[23] The essential point here is that the InAs WL lowers the energy of the e_1, hh_1, and lh_1 levels considerably, while leaving the energy of the e_2 level unaffected due to the antinode in its wave function

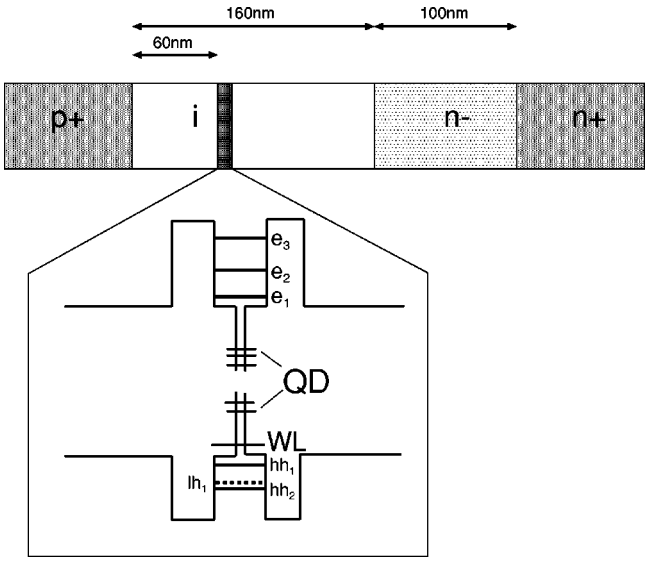

FIG. 1. Structure of the *p-i-n* diode. Inset: schematic band diagram of the double barrier structure with embedded QD's neglecting space charge effects. (e_1, e_2, e_3, ... electron quantum well states; hh_1, hh_2, ... heavy hole quantum well states; lh_1, ... light hole quantum well state.)

(upper electron and hole QW states are not considered here and not shown in the figure).

To carry out the two-terminal electrical measurements, samples were processed into circular mesas of 100–400 μm diameter. The *I-V* curves were taken on an HP4145B Semiconductor Parameter Analyzer configured to input a voltage sweep while measuring current.

III. EXPERIMENTAL RESULTS

The helium temperature *I-V* curve of a 100-μm diameter structure depicted in Fig. 2 is recorded by sweeping the voltage from 0 to 2.5 V and then back down to 0 V, while measuring the current through the device. The arrows in the figure show the predicted positions for resonances through electron and hole quasi-bound levels in the GaAs QW (compare the inset of Fig. 1). A pronounced hysteresis is displayed in the figure around a voltage of 2.3 V with the upper current branch corresponding to the voltage up sweep, see the lower inset of Fig. 2. The observation of the hysteresis in the *I-V* curve indicates a *Z*-shaped bistability in the device current for a given applied bias range. Precise measurements also reveal another region of double-valued current behavior at voltages between 1.2 and 1.4 V (see also Ref. 24). This feature becomes more visible with decreasing temperature. The upper inset in Fig. 2 represents the low bias portion of the *I-V* curve measured at 30 mK. The lower current branch now corresponds to the bias sweep up.

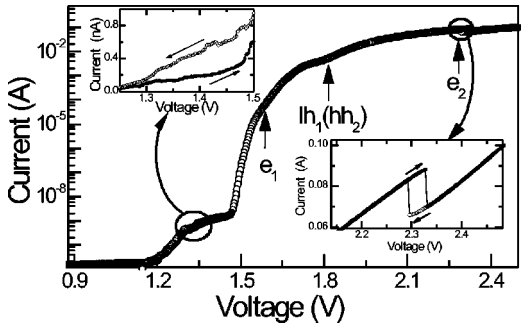

FIG. 2. Measured current-voltage characteristics of the DBRT ($T=4$ K). Solid (open) circles correspond to sweeping the voltage up (down). Labeled arrows correspond to predicted resonances by quantum well states e_1, e_2, lh_1, and hh_2. The upper (30 mK) and lower insets depict the first (inverted behavior) and second hysteresis loop, respectively.

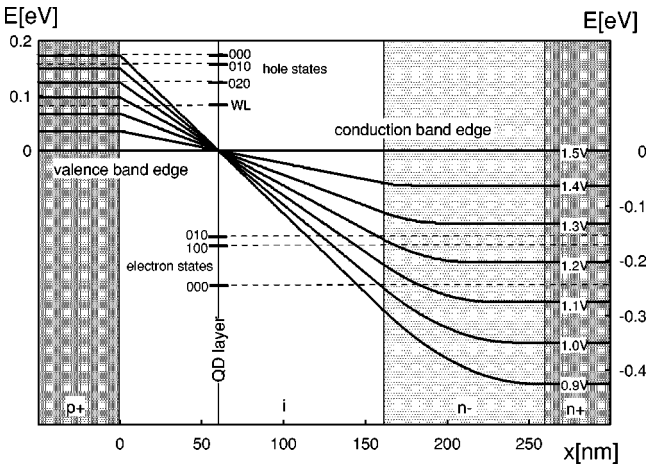

FIG. 3. Calculated band scheme in depletion approximation for different bias voltages. Electron and hole energies are counted upwards and downwards, respectively, from the solid lines. (The bandgap is removed in that scheme.) Electron and hole states in the pyramidal QD's (base length: 17 nm) are denoted by three quantum numbers. These states and the WL state lie in the band gap, and are taken from Ref. 25.

Now, let us examine the different processes contributing to the current flow. At low temperature and bias below the flat band condition, the main contribution to the current arises from the hole and electron tunneling into the *i* region and their subsequent recombination. The calculated band structure in the depletion approximation of the diode is shown in Fig. 3 in a bias range from 0.9 to 1.5 V. Since the quasi-Fermi energies in the highly doped p^+ and n^+ regions lie at $E_F^p \simeq 12$ meV and $E_F^n \simeq 140$ meV,[33] respectively, the current onset in the experiment is given by the tunneling of electrons into the QD states and of holes into the WL in the bias range considered. It appears that for V$>$1.2 V the QD hole states are above the band edge of the p^+ contact and thus they do not contribute to the tunneling current from the p^+ contact. The QD and WL states indicated in Fig. 3 are taken from Ref. 25 for a QD with a base length of 17 nm. This ladder of states as well as the base length is in reasonable agreement with previous photoluminescence, electroluminescence, and magneto-tunneling experiments (not presented here).

The appearance of the *S*-shaped bistability below the flat-band regime may be related to the charging of QD states. This situation is similar to the findings reported in Refs. 20,22. In addition we observe the standard *Z*-shaped

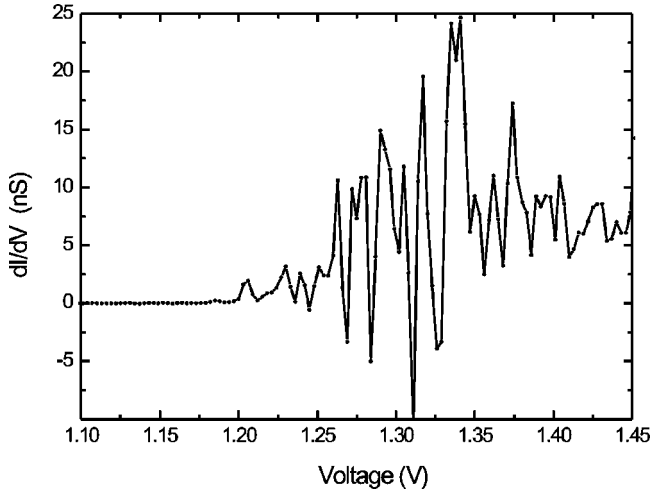

FIG. 4. Measured differential conductance vs bias voltage for $T=4$ K.

bistability[14,15,21] around 2.3 V, which seems to be related to the resonance between the excited electron level $e2$ and the n contact. Thus, it is possible in a p-n (or p-i-n) junction structure that the resonant tunneling conditions for electrons and holes are separated in applied bias voltage and can be controlled independently.

The key observation in the bias range from 1.1 to 1.45 V, i.e., below flat-band condition, is a quasi-periodic series of peaks in differential conductance. Figure 4 shows the differential conductance versus applied voltage measured at helium temperature (voltage sweep-up direction). The conductance oscillates with a period of approximately 10 mV indicating charging effects within the QD ensemble. These oscillations were observed in all mesas with different diameters and are fully reproducible.

IV. THEORY

In the following we address the observation of differential conductance oscillations and develop a model incorporating the relevant transport processes through the QD array. For unipolar resonant tunneling through QD arrays a master equation model has been developed.[10,11] In Ref. 12 we have extended this approach to the bipolar case applicable to the device considered here. We present the results of our simulations and compare them with the experimental data.

By using a master equation for the stationary occupation probability of the many-particle state $\nu=(n_1,\ldots,n_i,\ldots,)$ of the QD ensemble[7,12] we calculate the recombination current and its derivative with respect to the bias voltage. Here $n_i\in\{0,1\}$ are the occupation numbers of the single-particle QD states i. In the simulations we use the hole WL states as well as the spin degenerate ground state (000) and two spin degenerate excited states (100)/(010) and (010)/(020) for electrons and holes, respectively.[25] The charging of the states is treated in Hartree approximation,[26] using wave functions calculated by $\mathbf{k}\cdot\mathbf{p}$ theory[25] and including an electrostatic coupling between different QD's by means of a capacitance matrix.[12,27].

TABLE I. Inverse capacitance matrix elements $(C^{-1})_{ij}$ in meV for an InAs QD ($\epsilon=15.1\epsilon_0$) with base length of 17 nm calculated with wave functions taken from Refs. 25,29.

	$e(000)$	$e(100)$	$e(010)$	$h(000)$	$h(010)$	$h(020)$
$e(000)$	25.91	22.17	22.18	23.47	20.61	20.40
$e(100)$		22.67	18.81	20.27	18.26	19.95
$e(010)$			22.48	22.42	21.61	19.46
$h(000)$				23.07	21.63	20.23
$h(010)$					21.53	19.31
$h(020)$						19.94

For the unscreened Coulomb interaction between QD's i and j at positions $\mathbf{r}_i$ and $\mathbf{r}_j$ the matrix elements are given by ($r_{ij}\equiv|\mathbf{r}_i-\mathbf{r}_j|$)

$$(C^{-1})^0_{ij}=\frac{e^2}{4\pi\epsilon_0\epsilon_{\rm bg}r_{ij}}, \tag{1}$$

where ϵ_0 and $\epsilon_{\rm bg}$ are the absolute and relative background permittivities, respectively. In order to include the effect of static screening by the two-dimensional hole WL, the capacitance matrix elements are modified as follows:[28]

$$(C^{-1})_{ij}=\frac{e^2}{4\pi\epsilon_0\epsilon_{\rm bg}}\int_0^\infty dq\,\frac{J_0(qr_{ij})}{\epsilon(q)},$$

with

$$\epsilon(q)=1+\frac{c}{q} \tag{2}$$

and

$$c=\frac{e^2m}{2\pi\epsilon_0\epsilon_{\rm bg}\hbar^2}\left[1+\exp\left(\frac{E^h_{WL}-E^p_F}{k_BT}\right)\right]^{-1},$$

where J_0 is the zero-order Bessel function, m is the effective mass of holes in the WL, and E^h_{WL} is the energy of the WL hole state. For $r_{ij}\gg 1/c$ Eq. (2) can be approximated by[28]

$$(C^{-1})_{ij}=\frac{e^2}{4\pi\epsilon_0\epsilon_{\rm bg}c^2}\,\frac{1}{r^3_{ij}}. \tag{3}$$

The matrix elements for the Coulomb interaction between different occupied states in the same QD are given in Table I.[29] The electron/hole energies including the nonlinear Coulomb charging are given by

$$\epsilon^{e/h}_i=E^{e/h}_i+\sum_{j\neq i}(C^{-1})_{ij}n_j-(1-\eta_{e/h})\ \ {\rm eV}, \tag{4}$$

where $E^{e/h}_i$ are the intrinsic single-particle energy levels, and $\eta_{e/h}$ is the fraction of the voltage drop across the barriers, which is bias voltage dependent.

The processes considered in our model are depicted in Fig. 5. We choose bias-independent tunneling rates Γ^e_i for electrons which we estimate by a Wentzel-Kramers-Brillouin method for the bias voltages where the respective states are

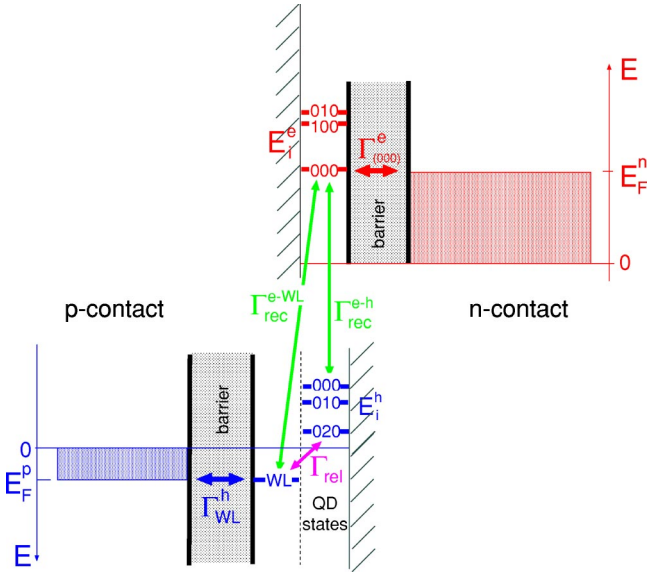

FIG. 5. Schematic energy diagram of the quantum dot structure, showing the relevant tunneling (Γ^e_i, Γ^h_{WL}), recombination ($\Gamma^{e\text{-}WL}_{rec}$, $\Gamma^{e\text{-}h}_{rec}$), and relaxation Γ^h_{rel} processes involving the hole WL and the electron and hole QD states.

filled: $\Gamma^e_{(000)}=10^6\ s^{-1}$, $\Gamma^e_{(100)}=10^7\ s^{-1}$, and $\Gamma^e_{(010)}=2\times10^7\ s^{-1}$. The hole WL is assumed to be in equilibrium with the *p*-contact. The recombination rates $\Gamma^{e\text{-}WL}_{rec}$ between electron QD states and hole WL state must be smaller than the electron tunneling rates because otherwise Coulomb charging features are not observable in the *I-V* characteristic. We choose $\Gamma^{e\text{-}WL}_{rec}=5\times10^6\ s^{-1}$ for all electron states. While we are not aware of direct experimental or theoretical evidence for this value, we motivate the use of such a small value (in comparison to typical recombination rates of electrons and holes in a QD $\Gamma^{e\text{-}h}_{rec}\sim10^9\ s^{-1}$)[30] as follows: The lowest bound states of electron and holes in the QD have typically a similar structure. Therefore the envelope function of the electron (000) state is approximately orthogonal to the envelope functions of the hole WL states. Thus the dipole matrix element between these states should be rather small suggesting $\Gamma^{e\text{-}WL}_{rec}\ll\Gamma^{e\text{-}h}_{rec}$.

First, we simulate the transport under the assumption that the QD hole levels are empty and the result is presented in Fig. 6. The QD ensemble contains 5×5 QD's which are arranged in a square lattice with equal nearest neighbor distances of 100 nm. The intrinsic single particle energy levels of electrons in a QD are $E^e_{000}=-250$ meV, $E^e_{100}=-175$ meV, and $E^e_{010}=-125$ meV (compare Fig. 3). The energy of the WL hole state is $E^h_{WL}=80$ meV and that of the QD hole states are $E^h_{020}=120$ meV, $E^h_{010}=170$ meV, and $E^h_{000}=190$ meV. The temperature in the simulations is set equal to 4 K.

The dotted curve in Fig. 6 gives our results for uniformly sized QD's taking into account the screening of the Coulomb interaction by the occupied WL state. At a bias of 1.04 V, the hole WL state starts to fill. At the same bias the electron ground state is singly occupied so that recombination takes place and a current is induced. The second step at 1.08 V is

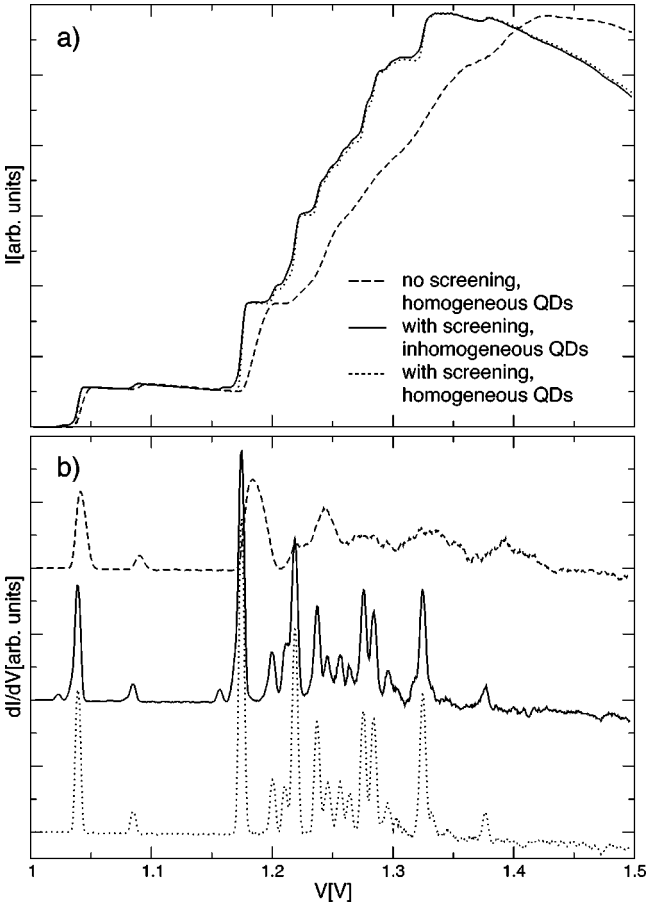

FIG. 6. (a) Calculated current-voltage characteristic for a periodic 5×5-quantum dot array. (b) Calculated differential conductance (curves are offset vertically for clarity). $T=4$ K, inter-QD distance: 100 nm, $\Gamma^{e\text{-}WL}_{rec}=5\times10^6\ s^{-1}$, $\Gamma^h_{rel}=0$, $\Gamma^{e\text{-}h}_{rec}=0$. Full curve: inhomogeneous QD's (10% size fluctuations), with screening; Dotted curve: homogeneous QD's (base length 17 nm), with screening; Dashed curve: inhomogeneous QD's, without screening.

caused by the double occupation of the spin degenerate electron ground state. The excited states start to fill at 1.17 V. The peaks in the differential conductance (Fig. 6) are caused by successive filling and charging of these many-particle states. Due to the uniformity of the QD's and the strongly screened Coulomb interaction between different QD's, each peak belongs to the occupation of the same state in each QD. Size fluctuations of the individual QD's change their intrinsic level spectrum and their charging energies (Table I). With an assumed size fluctuation of 10% and a screened Coulomb interaction, the peaks [full curve in Fig. 6(b)] become less pronounced but remain resolvable. The influence of an unscreened Coulomb interaction is shown in the dashed curves in Fig. 6. The *I-V* characteristic broadens and the peaks caused by charging of individual QD states disappear even if the QD's are uniform.

In the preceding paragraph we found that the occupation of electron QD states produces Coulomb charging peaks in the differential conductance. The same argument holds good for the hole QD states, which can be filled by relaxation from the hole WL state and hence can contribute to the current by recombination with the electron QD states. The associated

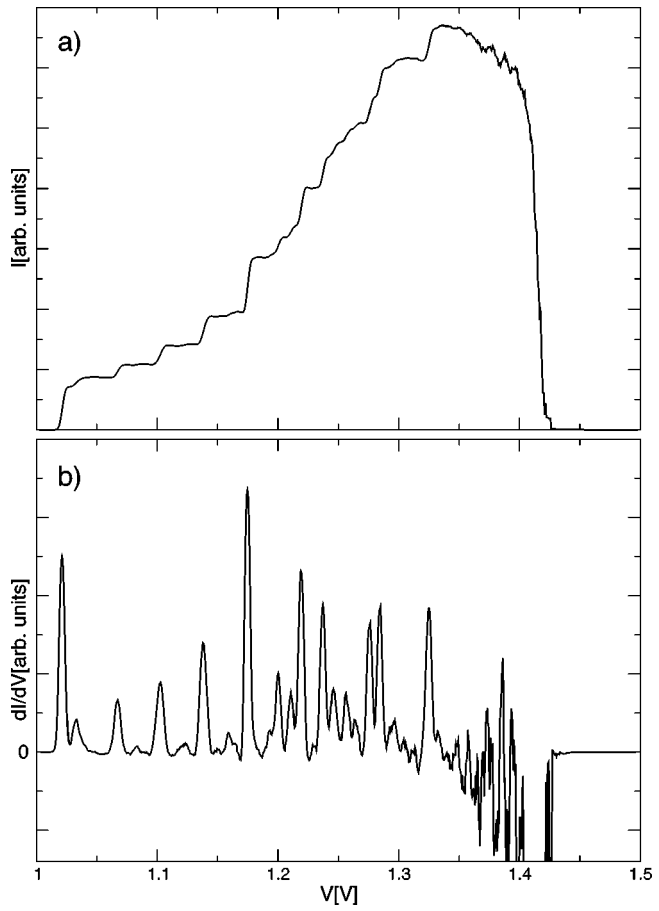

FIG. 7. (a) Calculated current-voltage characteristic for a 5×5-QD array with QD electron-hole recombination included. (b) Calculated differential conductance. $T=4$ K, inter-QD distance: 100 nm, with screening, $\Gamma_{\mathrm{rec}}^{e\text{-}h}=10^9\ \mathrm{s}^{-1}$, $\Gamma_{\mathrm{rel}}^{h}=5\times10^5\ \mathrm{s}^{-1}$.

recombination rate for radiative recombination is typically $\Gamma_{\mathrm{rec}}^{e\text{-}h}=10^9\ \mathrm{s}^{-1}$ as measured by time-resolved photoluminescence experiments.[30] The rate for relaxation of holes from the WL in the QD states is chosen as $\Gamma_{\mathrm{rel}}^{h}=C_{hh}n_hN_{QD}\approx5\times10^5\ \mathrm{s}^{-1}$ which we have estimated by the Auger capture coefficient $C_{hh}\approx5\times10^{-16}\ \mathrm{cm}^4/\mathrm{s}$ taken from Ref. 31 and a hole concentration in the WL of $n_h\approx10^{11}\ \mathrm{cm}^{-2}$, and using the QD density $N_{QD}=10^{10}\ \mathrm{cm}^{-2}$.[34] The result of this simulation is shown in Fig. 7 for an uniformly sized 5×5-QD array with screened Coulomb interaction. A comparison with the curves of Fig. 6 shows that additional differential conductance peaks occur due to Coulomb charging effects resulting from the occupation of hole QD states. The average period of the differential conductance oscillations becomes smaller and comparable with the experimental value. Due to the attractive Coulomb interaction between electrons and holes in the QD's the electron levels shift to lower energies so that above 1.4 V no electron QD states are available for tunneling and the current vanishes [Fig. 7(a)]. To avoid this effect higher excited electron states must be included in the simulations.

In summary, the simulations can reproduce the differential conductance oscillations in the experiment under the following assumptions: (i) The Coulomb interaction between different QD's is strongly screened by the holes in the WL; (ii) The size fluctuations of individual QD's are smaller than the intrinsic level spacing and the Coulomb charging energies; (iii) The recombination rate between the hole WL state and electron QD states is smaller than the tunneling rates, i.e., the lifetime of carriers in certain states has to be long enough so that they can experience Coulomb attraction or repulsion and charging effects can be observed.

Hence, we suggest that the observed differential conductance oscillations can be explained by the charging of individual QD's. These oscillations reflect the energy separation of different charging states including both holes and electrons as given by the inverse capacitance matrix elements in Table I.

V. CONCLUSIONS

We have carried out experimental and numerical investigations of bipolar transport in a *p-i-n* double barrier diode with a layer of self-organized InAs QD's embedded in the intrinsic region. The observed differential conductance oscillations were analyzed within a master-equation approach. We found reasonable agreement with the experiment under the assumption of strongly screened Coulomb interaction between neighboring QD's by the holes in the WL, and relatively small size fluctuations of the QDs. We suggest that the observed oscillations are caused by the Coulomb charging of different many-particle states including electrons and holes in the individual QDs. Furthermore, both an *S*-shaped and a *Z*-shaped current bistability is observed in the structure.

ACKNOWLEDGMENTS

A.E.B. acknowledges the Royal Society (U.K.) and the Deutsche Forschungsgemeinschaft (Germany) for financial support. S.A.V. thanks the support of the Office of Naval Research Grant No. 00014-00-1-4054. Furthermore, this work was supported by Deutsche Forschungsgemeinschaft in the framework of Sfb 296.

*Electronic address: kieslich@physik.tu-berlin.de; Fax: +49-(0)30-314-21130.

†On leave from the Institute of Semiconductor Physics, NASU, 03028 Kiev, Ukraine.

[1] *Single Charge Tunneling*, Vol. 294 of *NATO Advanced Study Institute, Series B: Physics*, edited by H. Grabert and M.H. Devoret (Plenum, New York, 1992).

[2] U. Meirav and E.B. Foxman, Semicond. Sci. Technol. **10**, 255 (1995).

[3] L.P. Kouwenhoven, C.M. Marcus, P.L. McEuen, S. Tarucha, R. M. Westervelt, and N.S. Wingreen, in *Mesoscopic Electron Transport*, edited by L.L. Sohn, L.P. Kouwenhoven, and G. Schön (Kluwer Academic Publishers, Dordrecht, 1997).

[4] I.E. Itskevich, T. Ihn, A. Thornton, M. Henini, T.J. Foster, P. Mo-

riarty, A. Nogaret, P.H. Beton, L. Eaves, and P.C. Main, Phys. Rev. B **54**, 16 401 (1996).
[5] M. Narihiro, G. Yusa, Y. Nakamura, T. Noda, and H. Sakaki, Appl. Phys. Lett. **70**, 105 (1997).
[6] I. Hapke-Wurst, U. Zeitler, H.W. Schumacher, R.J. Haug, K. Pierz, and F.J. Ahlers, Semicond. Sci. Technol. **14**, L41 (1999).
[7] C.W.J. Beenakker, Phys. Rev. B **44**, 1646 (1991).
[8] D.V. Averin, A.N. Korotkov, and K.K. Likharev, Phys. Rev. B **44**, 6199 (1991).
[9] G. Klimeck, R. Lake, S. Datta, and G.W. Bryant, Phys. Rev. B **50**, 5484 (1994).
[10] G. Kießlich, A. Wacker, and E. Schöll, Physica B **314**, 459 (2002).
[11] G. Kießlich, A. Wacker, and E. Schöll, Physica E (Amsterdam) **12**, 837 (2002).
[12] G. Kießlich, A. Wacker, and E. Schöll, Phys. Status Solidi B **234**, 215 (2002).
[13] R. Tsu and L. Esaki, Appl. Phys. Lett. **22**, 562 (1973).
[14] V.J. Goldman, D.C. Tsui, and J.E. Cunningham, Phys. Rev. Lett. **58**, 1256 (1987).
[15] A.D. Martin, M.L.F. Lerch, P.E. Simmonds, and L. Eaves, Appl. Phys. Lett. **64**, 1248 (1994).
[16] E. Schöll, *Nonlinear Spatio-Temporal Dynamics and Chaos in Semiconductors* (Cambridge University Press, Cambridge, 2001).
[17] A. Zaslavsky, V.J. Goldman, D.C. Tsui, and J.E. Cunningham, Appl. Phys. Lett. **53**, 1408 (1988).
[18] E.S. Alves, L. Eaves, M. Henini, O.H. Hughes, M.L. Leadbeater, F.W. Sheard, G.A. Toombs, G. Hill, and M. Pate, Electron. Lett. **24**, 1190 (1988).
[19] A.E. Belyaev, S.A. Vitusevich, B.A. Glavin, R.V. Konakova, T. Figielski, A. Makosa, L.N. Kravchenko, and W. Dobrowolski, Inorg. Mater. **33**, 116 (1997).
[20] P.A. Harrison, L. Eaves, P.M. Martin, M. Henini, P.D. Buckle, M.S. Skolnick, D.M.V. Whittaker, and G. Hill, Surf. Sci. **305**, 353 (1994).
[21] M. P. Shaw, V.V. Mitin, E. Schöll, and H.L. Grubin, *The Physics of Instabilities in Solid State Electron Devices* (Plenum Press, New York, 1992).
[22] O. Kuhn, J. Genoe, D.K. Maude, J.C. Portal, L. Eaves, M. Henini, G. Hill, and M. Pate, Physica E (Amsterdam) **2**, 483 (1998).
[23] A. Patanè, A. Polimeni, L. Eaves, P.C. Main, M. Henini, A.E. Belyaev, Yu.V. Dubrovskii, P.N. Brounkov, E.E. Vdovin, Yu.N. Khanin, and G. Hill, Phys. Rev. B **62**, 13 595 (2000).
[24] A.E. Belyaev, L. Eaves, S.A. Vitusevich, P.C. Main, M. Henini, A. Förster, N. Klein, and S.V. Danylyuk, in *Proceedings of 25th International Conference on the Physics of Semiconductors (ICPS-25), Osaka 2000*, edited by N. Miura (Springer, Berlin, 2001).
[25] O. Stier, M. Grundmann, and D. Bimberg, Phys. Rev. B **59**, 5688 (1999).
[26] R.J. Warburton, B.T. Miller, C.S. Dürr, C. Bödefeld, K. Karrai, J.P. Kotthaus, G. Medeiros-Ribeiro, P.M. Petroff, and S. Huant, Phys. Rev. B **58**, 16 221 (1998).
[27] C.B. Whan, J. White, and T.P. Orlando, Appl. Phys. Lett. **68**, 2996 (1996).
[28] T. Ando, A.B. Fowler, and F. Stern, Rev. Mod. Phys. **54**, 437 (1982).
[29] A. Schliwa and O. Stier (private communication).
[30] W. Yang, R.R. Lowe-Webb, H. Lee, and P.C. Sercel, Phys. Rev. B **56**, 13 314 (1997).
[31] A.V. Uskov, J. McInerney, F. Adler, H. Schweizer, and M.H. Pilkuhn, Appl. Phys. Lett. **72**, 58 (1998).
[32] S. Raymond, K. Hinzer, S. Fafard, and J.L. Merz, Phys. Rev. B **61**, 16 331 (2000).
[33] The quasi-Fermi levels are calculated from $E_F^n = [\hbar^2(3\pi^2 n)^{2/3}]/(2m_n)$, $E_F^p = [\hbar^2(3\pi^2 p)^{2/3}]/(2m_p)$ where n and p denotes the electron and hole concentration, respectively, and $m_n = 0.063m_e$ and $m_p = 0.5m_e$ are the effective masses for electrons and holes in GaAs, respectively.
[34] Note that it is still controversal in the literature whether this capture coefficient is too small by comparison with experimental data, see, e.g., Ref. 32.